Simulation of Semiconductor Processes and Devices 2016
Edited by E. Bär, J. Lorenz, and P. Pichler

Accurate IGBT Modeling under High-Injection Condition

A. Tone, Y. Miyaoku, M. Miura-Mattausch
U. Feldmann, H. Kikuchihara, H. J. Mattausch
Graduate School of Advanced Sciences of Matter
Hiroshima University
Higashi-Hiroshima, Japan
Email: m155574@hiroshima-u.ac.jp

D. Navarro
Silvaco Japan
Yokohama, Japan

***Abstract*— A compact model of IGBT (Insulated-Gate Bipolar Transistor) is developed by considering the high-injection condition explicitly. The model distinguishes the MOSFET controlled part and the bipolar transistor controlled part explicitly by introducing internal potential nodes, which are solved iteratively. It is verified that the model calculates the potential distribution along the device identical to that of 2D-device numerical simulation results. It is demonstrated that accurate and stable switching simulation is realized with the developed model.**

Keywords*— IGBT; compact model; high injection condition; potential distribution; resistance model

I. Introduction

The demand for high-power devices in various applications is increasing, which leads to the serious necessity of stable and predictive circuit simulation for sufficient design productivity [1]. A prerequisite to fulfill this application demand is therefore the realization of accurate circuit-simulation capability with the specific high-power device for any type of application. Here, we focus on achieving this task in case of the IGBT device, where high voltage operation even up to 10kV has been verified through utilization of advanced materials [2]. Since the IGBT structure can realize low on-resistance and at the same time fast switching in spite of high driving bias conditions, it is widely used in power conversion circuits, for example, motor control of electrical vehicles.

The IGBT internally consists of a MOSFET and a bipolar transistor, aiming at the realization of fast switching (see Fig. 1) [3]. The highly resistive base region can sustain extremely high applied voltages. This causes numerical instability due to the steep electric-field increase within the base. The compact model HiSIM-IGBT1, which is successfully utilized in industry, has been developed based on the potential distribution along the IGBT structure [4]. The core part of the resistivity is modeled by the carrier distribution within the base. However, the high injection condition is not explicitly considered in the modeling, which requires phenomenological description of the effect.

The new generation compact modeling of IGBT is done by explicitly considering the high-injection condition together with the ambipolar effect. Accurate prediction of the potential distribution within the IGBT, while preserving the consistency of the compact model description, is the key of our method. It is demonstrated that the presented approach enables straightforward compact IGBT modeling and achieves stable circuit simulation. It is further found that the amplification factor in the IGBT is normally equal to 1.3 under the high-injection condition, which exactly corresponds to the ratio of electron to hole mobility.

II. Modeling High Injection Condition

Fig. 1 shows the studied IGBT structure together with the equivalent circuit. The internal nodes b and b' describe the end of the gate control and the end of the resistive part for the injected carriers from the IGBT collector, respectively. Thus these nodes consider the mutual interaction of electrons from MOSFET and holes from bipolar part explicitly, which are used to describe the high injection condition correctly. Namely, the electron injection from the MOSFET part is influenced by the hole density arriving at the channel/base junction, where the injected electrons are controlled again by the resistance effect in the base region. In this way, the high-injection condition is effectively considered to balance the carrier distribution by considering the internal nodes.

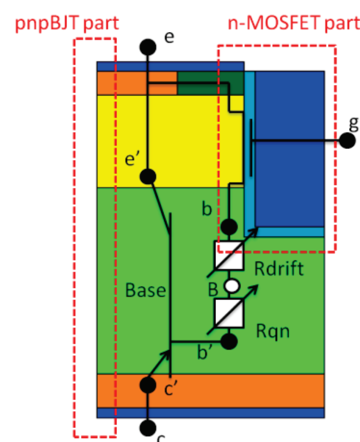

Fig. 1. Studied IGBT structure (nMOSFET + pnp bipolar part) with its corresponding simplifield equivalent circuit.

978-1-5090-0818-6/16/$31.00 ©2016 IEEE

The base current of the Bipolar Junction Transistor (BJT) is supplied by the drain current of the MOSFET and the BJT's emitter current (collector current of IGBT) supplies holes to the collector (emitter of IGBT). Fig. 2 compares a 2D-device simulation result of the I_c-V_c characteristics of a bipolar device and an IGBT structure. It is noticeable that high injection occurs even at very low bias conditions for the IGBT, without clear exponential relationship, a typical BJT characteristic. Fig. 3 compares 2D numerical device simulation results of the carrier distribution within the IGBT for two different applied collector-emitter bias V_{ce} conditions of 0.2V and 15V. It is seen that the electron density injected from MOSFET to the base of BJT is negligibly small under the low injection condition. It distributes in the same way as holes, which are injected from the collector after the Shockley equation. Namely, carriers are controlled by the diffusion mechanism.

Under the high-injection condition, the carrier density injected from MOSFET to BJT base easily exceeds the impurity concentration, resulting in increased hole concentration at the same time. This means, that the BJT carrier distribution is no more represented by an ideal exponential equation, as derived by Shockley under the diffusion approximation, which is applicable only for the hole injection at the collector/base junction. Under high injection, however, electron and hole concentrations remain equal, which establishes a clear ambipolar condition again, as in low injection.

Fig. 3b shows that the carrier distribution within the base is much flatter under the high-injection condition than that predicted by the Shockley equation. As shown in Fig.4, the electron and the hole current flowing in the base region of IGBT are mostly governed by the drift mechanism. This is because the potential applied is mostly consumed within the base region, resulting in the high field. This concludes that the largest potential drop occurs between the two internal nodes "b" and "b' ". Though the electron and the hole density within the base are the same, however, the electron current density is three times larger than that of the holes. The difference is attributed to the mobility difference. The electron current injected from the MOSFET is written as [5]

$$I_{ds} = \frac{W_{eff}}{L_{eff}} \mu_e \frac{I_{dd}}{\beta} \tag{1}$$

$$I_{dd} = C_{ox}(\beta V_g' + 1)(\phi_{SL} - \phi_{S0}) - \frac{\beta}{2} C_{ox}(\phi^2{}_{SL} - \phi^2{}_{S0})$$
$$- \frac{2}{3} const0[(\beta\phi_{SL} - 1)^{3/2} - (\beta\phi_{S0} - 1)^{3/2}]$$
$$+ const0[(\beta\phi_{SL} - 1)^{1/2} - (\beta\phi_{S0} - 1)^{1/2}]$$

where I_{ds} is drain current of the MOSFET part, W_{eff} is channel width, μ_e is the electron mobility in the base region, L_{eff} is effective channel length, C_{ox} is oxide capacitance, β is the inverse of the thermal voltage, ϕ_{sl} is the potential at the pinch-off point and ϕ_{s0} is the surface potential at the source side. Due to the ambipolar effect, the carrier concentrations are equal and the mobilities are different for electrons and holes. Thus the BJT's collector current under high injection can be written as

$$\frac{I_e}{\mu_h} = \frac{I_{ds}}{\mu_e} \Rightarrow I_e = \frac{\mu_h}{\mu_e} I_{ds} \tag{2}$$

where μ_h is the hole mobility. With the Kirchhoff law, the amplification factor I_c/I_b (=I_{ds}) is denoted by the mobility ratio as

$$\frac{I_c}{I_b(=I_{ds})} \approx 1.3 \tag{3}$$

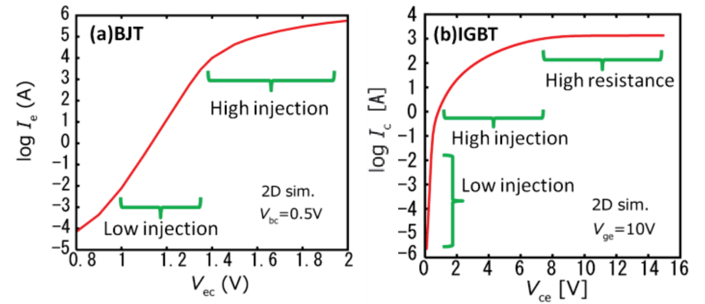

Fig. 2. 2D-device simulation result of I_c vs. V_{ce} for (a) BJT and (b) IGBT.

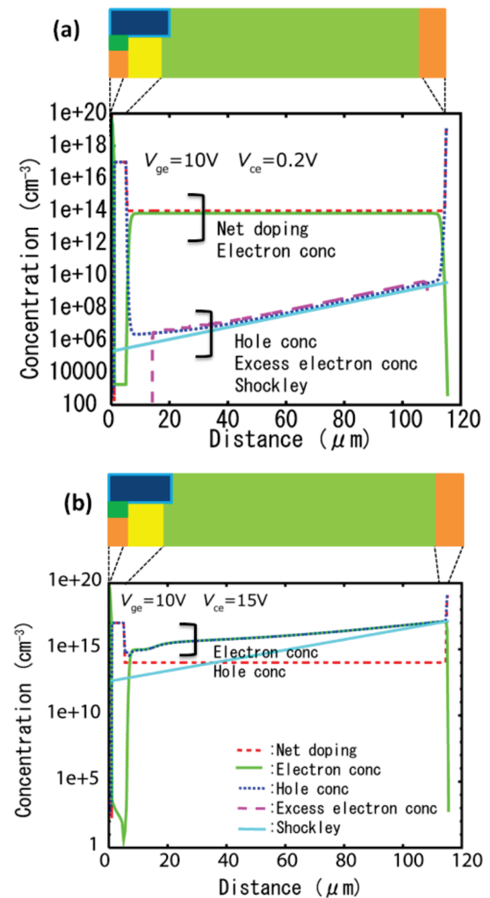

Fig. 3. 2D-device simulation results of electron- and hole concentration distribution along the base region, (a) for V_{ce} =0.2V and (b) for V_{ce} =15V.

The collector current is written as [6]

$$I_c = Aq\frac{D_b p_b}{L_b}\coth(\frac{W_{base}}{L_b})[(\exp(\frac{qV_{cb'}}{kT})-1)-\frac{\exp(qV_{eb}/kT)-1}{\cosh(W_{base}/L_b)}] + Aq\frac{D_c n_c}{L_c}(\exp(qV_{cb'}/kT)-1) \quad (4)$$

where D_b, p_b and L_b are diffusion coefficient, hole concentration and diffusion length in the base region, D_c, n_c and L_c are diffusion coefficient, hole concentration and diffusion length in the collector region, W_{base} is base length, k is Boltzmann's constant and T is temperature. This equation is equal to that of the BJT emitter current derived by Shockley.

III. Modeling Resistance Effect

As shown in Fig.5, the gate voltage affects the potential distribution in the base region. In the equivalent circuit shown in Fig. 1, therefore, two resistances are considered independently, namely R_{drift} and R_{qn}. The carrier density injected from MOSFET is strongly influenced by R_{drift}. This is because the resistance is determined by the gate voltage as well as the potential drop between the node "b" and "B", which is referred to as the drain voltage of the MOSFET part. The carrier density injected from the collector is determined by the node potential "b' " and is influenced by the resistance R_{qn}. The model equations of HiSIM_HV for power MOSFETs are adopted for R_{drift} as [7]

$$R_{drift} = W_{eff}X_{ov}qN_{drift}\mu_{drift}\frac{V_{Bb}}{L_{drift}+\mathrm{RDRDL1}} \quad (5)$$

where W_{eff} is channel width, X_{ov} is current path width, N_{drift} is base concentration, μ_{drift} is mobility in the drift region, L_{drift} is length of drift resistance and RDRDL1 is effective L_{drift} of current in drift region. The equation is derived by considering the current flow within a resistor. The BJT resistance (R_{qn}) is written by carrier distribution injected from the collector as

$$R_{qn} = \frac{1}{\mu_e+\mu_h}\frac{L_{dec}}{q_{ex,A}+AqN_{base}}(\exp(\frac{W_{qn}}{L_{dec}})-1) \quad (6)$$

where L_{dec} is diffusion length in the base region, $q_{ex,A}$ is charge injected from collector, A is cross-section area, N_{base} is concentration in the base region and W_{qn} is width of the quasi-neutral region. L_{drift} and W_{qn} are written by depletion length as

$$L_{drift} = \alpha\sqrt{\frac{2\varepsilon_{si}}{q}\frac{V_{ce}}{N_{base}+p_{dep0}+p_{ex,K}}} \quad (7)$$

$$W_{qn} = W_{base} - L_{drift} \quad (8)$$

where α is balance coefficient of width of depletion and the quasi-neutral region, p_{dep0} is hole density in the depletion region, $p_{ex,K}$ is charge injected from emitter and W_{base} is base length.

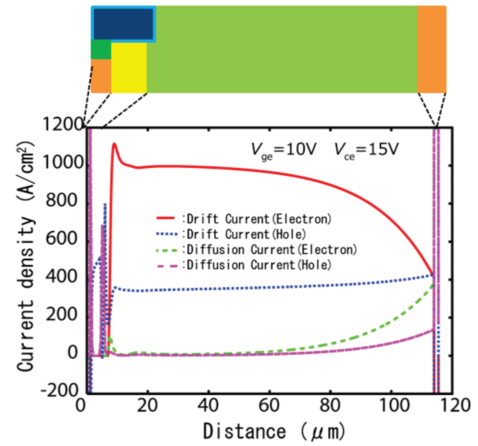

Fig. 4. 2D-device simulation results of individual current density distributions at V_{ge}=10Vand V_{ce}=15V.

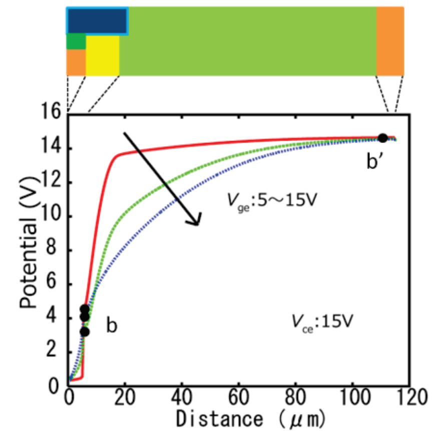

Fig. 5. 2D-device simulation results of potential distribution depending on V_{ge}. Solid circles are calculated node potentials at "b", "B", and "b' " with the developed model.

IV. Comparison with 2D Device Simulation Results

The newly developed IGBT compact-model is named HiSIM-IGBT2. Fig. 6 compares HiSIM-IGBT2 calculation results to 2D device simulation results under different operating conditions. Fig. 7 compares node-potential difference V_{be} (b-e) and $V_{bb'}$ (b-b') calculated with HiSIM-IGBT2 and 2D device simulation results. It is seen that the developed model reproduces the potential distribution within the device accurately. This proves that the partitioning into the MOSFET contribution part and that of BJT is accurately done. It is also seen that applied voltages are sustained mostly within $V_{bb'}$. However, the potential node B moves from near to "b" to "b' " because of the MOSFET and BJT characteristics. Thus, it can be explained that the potential drop between b and b' node is dominated by BJT resistance R_{qn} when V_{ce} is low. When V_{ce} becomes high, however, the potential drop between b and b' node is dominated by MOSFET resistance R_{drift}. This dynamic feature of IGBT can be well reproduced by the developed model.

Fig. 8 shows the comparison of transient simulation results with HiSIM-IGBT2 and 2D-device simulation. For the simulation, a pulse is applied on the gate electrode while keeping the drain voltage V_{cc} constant. The circuit used for the simulation is shown in Fig. 8b. The element values taken typically appear in literature. A typical freewheel diode is applied. The agreement is quite satisfactory. The long tail observed in V_{ge}, the internal node potential of the gate, is due to the gate capacitance and resistance. The good agreement of V_{ge} verifies accurate modeling of, not only the currents but also capacitances.

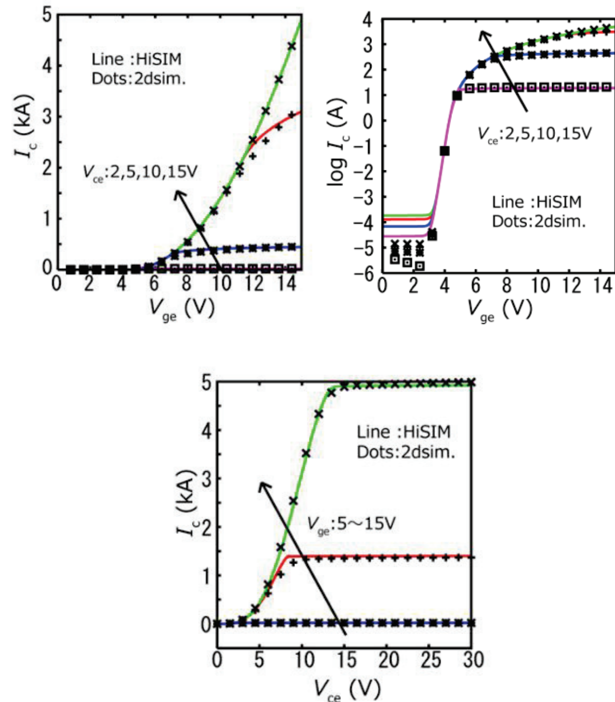

Fig. 6. Calculated *I-V* characteristics in comparison to 2D device simulation results.

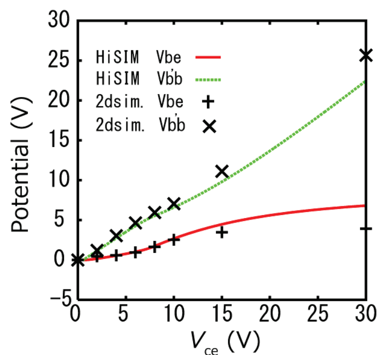

Fig. 7. Comparison of modeled node-potential differences Vbe (b-e) and Vb'b (b-b') to those of 2D-device simulation results.

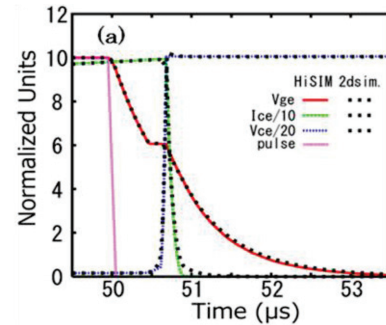

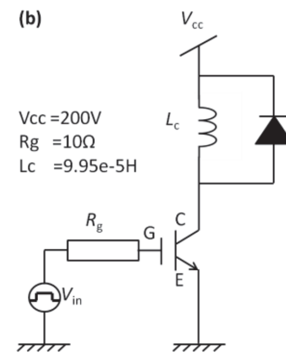

Fig. 8. (a) Transient simulation results of HiSIM-IGBT2 compared with the 2D-device simulation results, (b) Test circuit.

V. CONCLUSION

The reported IGBT compact model is based on high injection condition, which considers injected electron and hole density in the base region as well as MOSFET and BJT contributions. Under high injection, electrons and holes in the base region are interrelated. Because electrons are injected from MOSFET and holes are injected from collector, it is necessary to consider the contribution of MOSFET and BJT in order to develop an accurate model. Newly developed model (HiSIM-IGBT2) is verified to reproduce various 2D device simulation results.

References.

[1] H. Ohashi, and I. Omura, "Role of Simulation Technology for the Progressin Power Devices and Their Applications," IEEE Trans. Electron devices, Vol. 60, No. 2, pp. 528-534, Feb. 2013.

[2] S.-H. Ryu, C. Capell, C. Jonas, L. Cheng, M, O'Loughlin, A. Burk, A. Agarwal, J. Palmour, A. Hefner, "Ultra High Voltage (>12kV), High performance 4H-SiC IGBTs," Proceeding of ISPSD2012, pp 257-260.

[3] B. J. Baliga, "Fundamentals of Power Semiconductor Devices," 2010

[4] M. Miyake, D. Navarro, U. Feldmann, H. J. Mattausch, T. Kojima, T. ogawa T. Ueta, "HiSIM-IGBT: A Compact Si-IGBT Model for Power Electronic Circuit Design," IEEE trans. Electron devices, Vol. 60, No. 2, pp. 571-579, Feb. 2013.

[5] M. Miura-Mattausch, H. J. Mattausch, and T. Ezaki, "The Physics and modeling of MOSFETs," World Scientific, Singapore, 2008.

[6] S. M. Sze, "Physics of Smiconductor Device 2nd Edition", p. 137, 1981

[7] HiSIM_HV 2.3.0 User's Manual, Hiroshima University, 2015.